CIMAC CONGRESS 25
ZURICH, MAY 19 – 23, 2025

2025 | 206

Mechanism development and combustion system study of low-speed two-stroke marine hydrogen engine

Basic research & advanced engineering - new concepts

Wenjing Qu, Dalian University of Technology

Yuan Fang, Dalian University of Technology
Liyan Feng, Dalian University of Technology

ABSTRACT

Due to the low ignition energy of hydrogen, hydrogen internal combustion engines are prone to pre-ignition. Therefore, modern hydrogen engines typically employ a lean combustion strategy. However, hydrogen also has a high auto-ignition temperature, necessitating additional ignition sources to provide sufficient energy for igniting ultra-lean mixtures and ensuring stable flame propagation. This is particularly crucial for low-speed two-stroke marine hydrogen engines (LTMHEs), which feature larger cylinder bores and leaner fuel/air mixtures.

This study uses primary reference fuel (PRF) as a surrogate for practical diesel fuel. The ignition delay times (IDTs) of n-heptane/hydrogen, iso-octane/hydrogen, and PRF/hydrogen mixtures were experimentally measured under high-pressure (8 bar, 16 bar, 24 bar) and low-temperature (600 K – 1000 K) conditions in a rapid compression machine, simulating engine conditions. A multi-objective genetic algorithm was employed to develop a new skeletal PRF/hydrogen mechanism, ensuring that the IDTs predicted by this enhanced mechanism closely match experimental data, thus ensuring the accuracy of the combustion model. Furthermore, the hydrogen jet flame characteristics were studied using an optical constant-volume combustion chamber (CVCC). The study investigates the effects of pre-chamber combustion on hydrogen jet flame behavior, providing insights for the combustion system design of LTMHEs.
Coupled with the skeletal hydrogen/PRF mechanism, engine performance under various combustion system designs for a low-speed two-stroke marine hydrogen/diesel engine with a 340 mm cylinder bore was analyzed through numerical simulations. The study compares the combustion characteristics of two ignition sources—spark ignition and pilot diesel ignition—and their respective positions (cylinder and pre-chamber). The results show that LTMHEs, utilizing the lean combustion strategy, require additional ignition energy to ignite the lean pre-mixture, like spark plugs or micro-pilot diesel injection. The pre-chamber widens the flammable limit of the lean pre-mixture, accelerates combustion, and improves combustion variability. Additionally, the risk of excessively high combustion temperatures can be mitigated, offering significant potential for enhancing power performance while controlling NOx emissions. Increasing the combustion intensity in the pre-chamber—through higher spark plug ignition energy, increased pilot diesel energy proportion, and enriched hydrogen injection—enhances jet flame combustion. To comply with stricter future emission regulations, pilot diesel ignition in the pre-chamber, with its significant potential for NOx reduction, is a promising solution.

1 INTRODUCTION

As a long-term renewable and less-polluting fuel, hydrogen exhibits clean combustion characteristics and superior performance, which have attracted significant attention. Marine Low-speed two-stroke hydrogen engines provide a significant solution on Greenhouse Gas (GHG) emissions and harmful emissions reductions for large ocean-going ships. However, the development of marine Low-speed two-stroke hydrogen engines is facing to great challenges.

The high auto-ignition temperature of hydrogen means that compression ignition is not practical in hydrogen engines. Therefore, it is necessary to provide additional ignition energy, like diesel pilot ignition or spark ignition (SI). Meanwhile, the extremely low ignition energy of hydrogen/air mixture leads to the inclination of pre-ignition in hydrogen internal combustion engines (ICEs), which has been mentioned in many research [1-4]. Pre-ignition is also considered as an important factor of knock. Thus, necessary measures must be taken to avoid these abnormal combustion phenomena. For the low-speed two-stroke marine hydrogen engines (LTMHEs), the super-large bore, extra-long stroke, ultra-low speed, and relatively high power density results in significant challenges in suppressing abnormal combustion. In modern hydrogen ICEs, the lean combustion strategy is commonly adopted to reduce the propensity for pre-ignition and knock. Firstly, to suppress the pre-ignition and knock, the excess air coefficient of hydrogen engines should be approximately 2.5 [5, 6]. Secondly, the homogeneity of the hydrogen/air pre-mixture before ignition should be improved as far as possible to prevent the local high concentration of hydrogen. To meet this requirement, the hydrogen injection system was designed in our previous study [7]. The effects of hydrogen injection timing and the arrangement of hydrogen injectors on pre-mixture homogeneity and hydrogen slip through the exhaust valves were investigated, resulting in the determination of an optimal hydrogen injection system design. Thirdly, the combustion system must be designed and optimized. As noted earlier, an additional ignition source is required to ignite the lean hydrogen/air mixture and achieve efficient lean combustion. This ignition source can be spark ignition or pilot diesel ignition. In addition to the lean pre-mixture, the large volume of the LTMHE combustion chamber significantly increases the difficulty of initiating combustion. Fortunately, in terms of achieving stable and reliable ignition and combustion, the pre-chamber has been widely demonstrated as a practical solution in many studies [8-10]. However, there is relatively little research on combustion system of LTMHE. Therefore, it is necessary to discuss the suitable combustion system design for LTMHE.

In this study, a serial of 3D CFD simulations on the engine working process were carried out to investigate the engine performance and optimize the combustion system of the LTMHE. Since the working process numerical simulations require an accurate combustion chemical mechanism, a skeletal hydrogen/diesel mechanism was developed, with primary reference fuel (PRF) selected to represent diesel in this study. Firstly, the ignition delay times (IDTs) of hydrogen/n-heptane, hydrogen/iso-octane, and hydrogen/PRF mixtures under engine conditions were measured using a rapid compression machine (RCM). Then, a multi-objective genetic algorithm was employed to automatically and efficiently optimize the reaction rate constants of the PRF mechanism from Liu [11] , ensuring that the IDTs predicted by the updated mechanism aligned with the experimental data. Secondly, the pre-chamber jet flame characteristics and their influence on the combustion of hydrogen were investigated by using an optical constant-volume combustion chamber (CVCC), and the results were used as the references for the combustion system design of hydrogen LTMHE. Finally, using the skeletal hydrogen/PRF mechanism developed, the combustion system of the LTMHE was designed through 3D CFD simulation referring to the experimental findings from the CVCC. Engine performance with two different ignition sources—spark ignition and pilot diesel ignition—at two different ignition positions (cylinder and pre-chamber) was studied. The feasibility and advantages of these different operating schemes were compared.

2 RCM EXPERIMENT

The IDTs of hydrogen/n-heptane, hydrogen/iso-octane, and hydrogen/PRF mixtures with varying hydrogen blending ratios, dilution ratios, and equivalence ratios under engine conditions (pressure of 8 bar, 16 bar, and 24 bar and temperature of 600 K–1000 K) were measured using the RCM [12-14] shown in Figure 1. The IDT is defined as the time from the end of compression to the point of peak dp/dt. The measured IDTs are presented in Figure 3.

To save computational time, a skeletal mechanism is required for 3D CFD simulations. Using the experimentally obtained volumetric traces, the IDTs under different operating conditions were calculated in Cantera [15]. In this study, a skeletal hydrogen/n-heptane oxidation mechanism was developed using a multi-objective genetic algorithm, which automatically and efficiently optimized some reaction rate constants of C7-C8

reactions in a PRF skeletal mechanism from Liu [11].

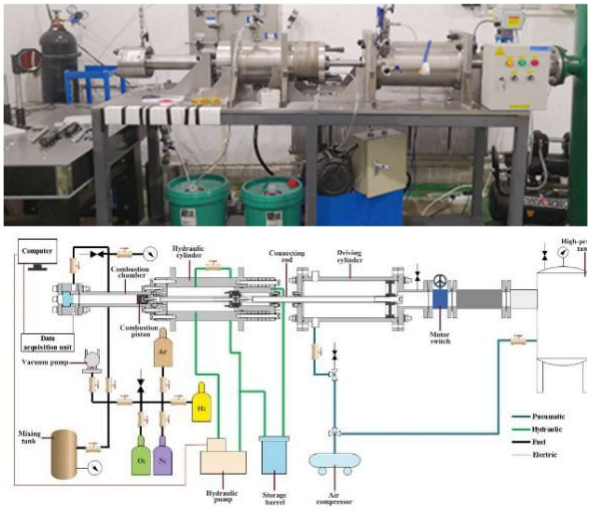

Figure 1. Physical picture and schematic of RCM.

The mechanism optimization flowchart is shown in Figure 2. The genetic algorithm (GA) has been proven highly effective for optimizing chemical mechanisms in high-dimensional pre-exponential factor parameter spaces [16]. The primary steps include initially defining the uncertainty range of the selected reactions manually, which is then translated into multipliers for the corresponding pre-exponential factors. Notably, for the optimization of reduced mechanisms, larger uncertainty ranges can often be employed due to the reduced mechanisms' simplified nature. These mechanisms omit many reaction pathways and utilize lumping techniques to combine reactions involving structural isomers. The target data for the GA optimization are derived from the current RCM IDTs experimental results. Specifically, for the RCM experimental data, volume traces from non-reactive experiments are incorporated to achieve more accurate IDTs in simulation calculations. The optimization process begins with the generation of an initial population comprising numerous individuals. Each individual's genetic code includes binary representations of multipliers for the reaction rate constants of all reactions to be optimized. Through repeated execution of genetic operations—such as crossover, mutation, and inheritance—the population is continually updated, with each individual evaluated using a fitness function. The process iterates until the fitness value meets the predefined convergence criteria, at which point the best individual is output as the optimization result.

As shown in Figure 3, the IDTs predicted by the Liu mechanism (dashed lines) differ significantly from the experimental results, particularly for mixtures with higher hydrogen blending ratios. In contrast, a remarkable improvement in prediction accuracy was achieved with the updated mechanism (solid lines). Thus, the present skeletal hydrogen/PRF oxidation mechanism was selected to perform 3D CFD simulations.

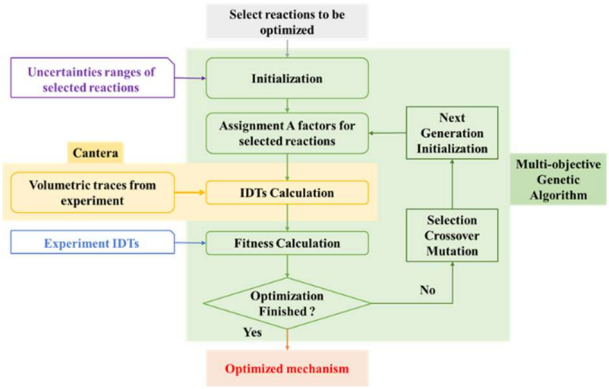

Figure 2. Mechanism optimization flowchart.

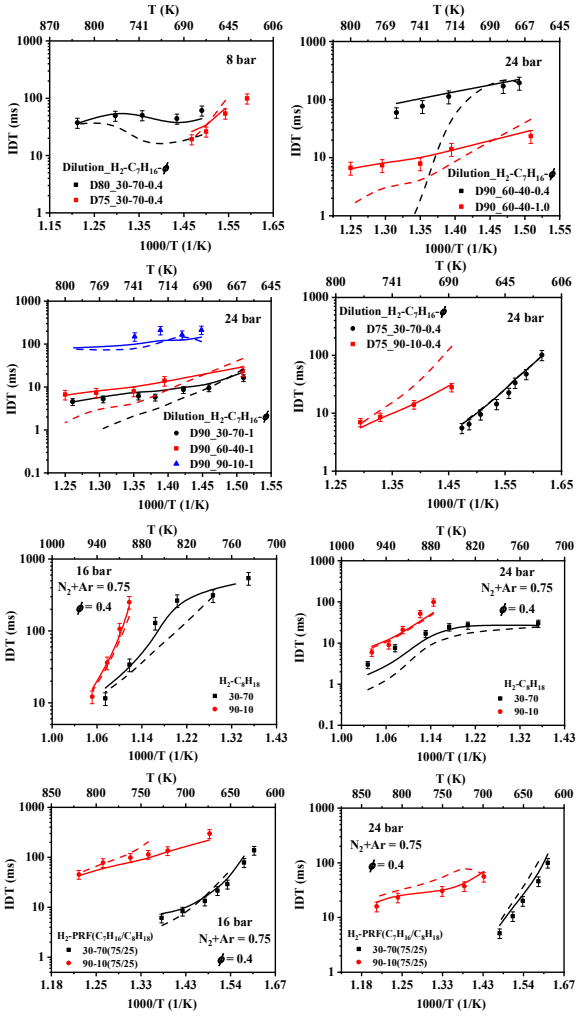

Figure 3. Comparison of the IDTs of the experimental results (points) and the simulated results based on the Liu mechanism [11] (dashed lines) and present mechanism (solid lines).

3 PRE-CHAMBER JET FLAME EXPERIEMNT

3.1 HYDROGEN JET FLAME

The characteristics of hydrogen jet ignition and combustion were investigated by measuring natural luminescence in the CVCC [17-20] (see Figure 4). The schematic of the CVCC is shown in Figure 5a. A spark plug integrated with a pressure sensor was installed at the upper part of the pre-chamber (see Figure 5b). The experiment revealed that, in addition to the brightness, width, and moment of emergence, differences in jet flame intensity were also reflected in the color.

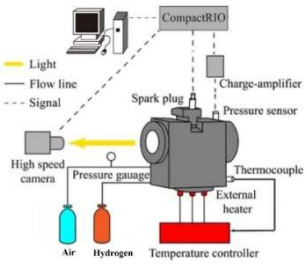

Figure 4. Schematic diagram of experimental setup.

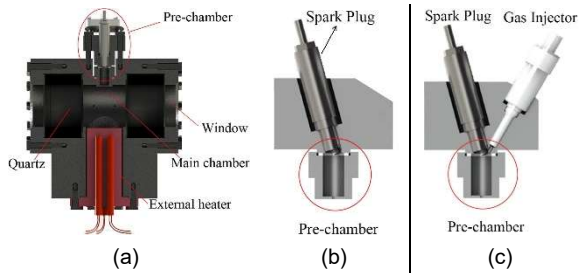

Figure 5. Schematic of CVCC.

As the jet flame intensity increases, the color of the jet flame changes from dark yellow to bluish violet and then to luminous yellow (Figure 6). The dark yellow and bluish violet colors are emitted by hydrogen combustion. The spectral lines emitted by hydrogen atoms include four wavelengths in the visible light spectrum: 410 nm, 434 nm, 486 nm, and 656 nm [21], corresponding to violet, blue, blue-green, and red, respectively (see Table 1).

On the other hand, intense combustion results in high-temperature flames, which exhibit shorter wavelengths. Thus, the dark yellow, superimposed by red and blue, indicates low hydrogen jet flame intensity. As flame intensity increases, the jet flame color shifts to bluish violet, resulting from the superposition of blue and violet. The luminous yellow is emitted by abundant water molecules in the excited state [22]. Water is the only direct product of hydrogen combustion. When sufficient hydrogen combusts, producing abundant water and generating enough heat, the water molecules absorb sufficient energy and transition to the excited state. Consequently, high-intensity hydrogen jet flames emit luminous yellow.

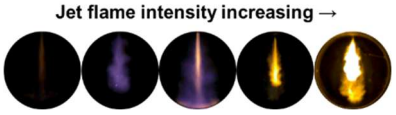

Figure 6. The comparison of color under different jet flame intensities.

Table 1. The spectral lines emitted by hydrogen atoms and responding color.

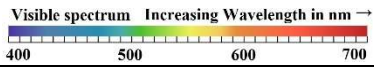

Name	H-α	H-β	H-γ	H-δ
Wavelength(nm)	410	434	486	656
Color	Violet	Violet	Blue	Red

3.2 ENRICHED HYDROGEN INJECTION IN PRE-CHAMBER

The jet flame plays a key role in combustion characteristics, so it is important to identify the influencing factors of hydrogen jet flames. The equivalence ratio in the pre-chamber directly affects the combustion in the pre-chamber, thereby determining the propagation velocity, burning temperature, and pattern of the hydrogen jet flame. Therefore, the effects of the equivalence ratio in the pre-chamber on the jet flame were studied. A gas injector was installed next to the spark plug at the top of the pre-chamber to supply hydrogen to the pre-chamber separately (see Figure 5c). The initial temperature was 300 K, and the initial pressure was 0.6 MPa. The volume and orifice diameter of the pre-chamber were 6 mL and 2 mm, respectively.

Figure 7 shows natural luminescence images of jet ignition processes in the main chamber with different equivalence ratios for the pre-chamber. The time shown in the figures starts from spark ignition, and the subsequent time is After Jet Appear (AJA). In the baseline condition, the equivalence ratios in the main chamber and the pre-chamber were both 0.4. In pre-chamber-enriched conditions, the equivalence ratio in the main chamber remained at 0.4, while the pre-chamber was enriched individually to equivalence ratios of 0.5, 0.7, and 1.0. It can be observed from Figure 7 that as ϕ increases in the pre-chamber, the intensity of the hydrogen jet flame initially increases and then decreases. The reason for this phenomenon is the quenching effect of the pre-chamber orifice. Combustion in the pre-chamber becomes more violent as fuel concentration increases. When the combustion becomes extremely violent (ϕ_{pre} = 1.0), the flame will be

quenched as it passes through the orifice. Accordingly, the jet flame intensity decreases [17, 23]. The same conclusion can also be drawn from Figure 8.

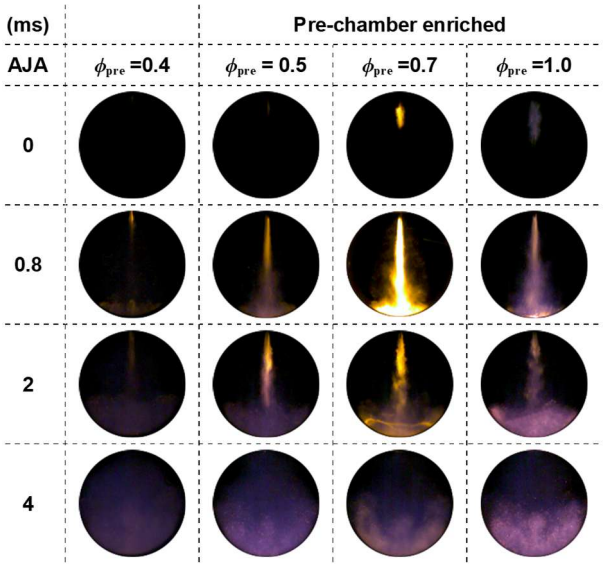

Figure 7. The images of hydrogen jet flame under different equivalence ratios in pre-chamber.

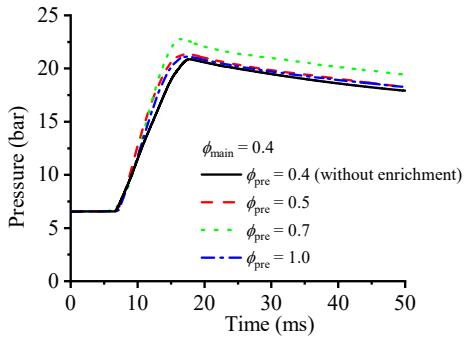

Figure 8. The comparison of pressure under different equivalence ratios in pre-chamber.

The maximum pressure and the pressure rise rate increase significantly after the equivalence ratio in the pre-chamber increases from 0.4 to 0.5 or 0.7. Before pre-chamber enrichment, the pressure peaks at 17.76 ms with a maximum pressure of 14.89 bar. With the pre-chamber enriched to equivalence ratios of 0.5 and 0.7, the peak pressure moment occurs 0.6 ms and 1.3 ms earlier, respectively. Additionally, the maximum pressure increases to 15.36 bar and 16.76 bar, respectively. However, further increasing the equivalence ratio in the pre-chamber to 1.0 is counterproductive. When the equivalence ratio in the pre-chamber is enriched to 1.0, the peak pressure decreases to 15.12 bar, and the peak pressure moment is delayed to 17.16 ms.

In conclusion, increasing the equivalence ratio appropriately in the pre-chamber can enhance the hydrogen jet flame. However, an overly enriched mixtures in pre-chamber results in a weakened jet flame. These findings provide guiding suggestion for combustion system of LTMHE with enriched pre-chamber design.

4 SIMUALITON OF LTMHE WORKING PROCESS

4.1 RESEARCH OBJECT AND MODEL

Coupled with the skeletal hydrogen/PRF mechanism, and referring to the hydrogen jet flame analysis obtained above, the 3D CFD simulation was conducted to design the combustion system in a LTMHE. The LTMHE was designed based on a low-speed two-stroke marine diesel engine. The basic and performance parameters under 100% load are shown in Table 2.

Table 2.Basic and performance parameters of the prototype diesel engine under 100% load.

Type	Parameter
Bore /mm	340
Stroke /mm	1600
Compression ratio (CR)	19.8
Rotate speed /rpm	157

Table 3. The sub-models of CFD simulation.

Model	Parameter
Turbulence model	RNG k-ε
Wall heat transfer model	O'Rourke and Amsden
Combustion model	SAGE
Spray breakup model	Blob model + KH-RT model
Emissions model	Extend zeldvoich (NOx), Nagel Strickland-Constable (soot)

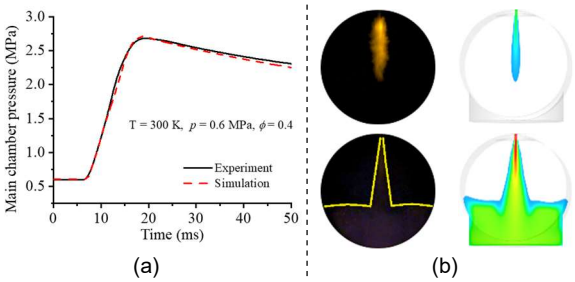

Figure 9. Model calibration of CFD simulation.

CONVERGE was used to establish the 3D CFD simulation model. The adaptive and regional mesh refinement strategies were set in the 3D model, and the mesh sensitivity analysis was carried out to ensure the rationality of the mesh refinement strategies and the basic grid size while avoiding inaccurate results caused by insufficient mesh

accuracy. Table 3 displays the sub-models used in the CFD simulation, which have been validated through the CVCC experiment (see Figure 9).

The compression ratio (CR) of low-speed two-stroke natural gas/diesel dual fuel engines is usually lower than 15 and around 13 [24-28]. Hydrogen has a more active chemical character and faster burning velocity. Thus, the CR of the LTMHE in this study is reduced from 19.8 to 13. In the process of combustion system design, the maximum in-cylinder pressure of the LTMHE is constrained to about 90% of the prototype diesel engine to ensure engine safety. Additionally, the lean combustion strategy was adopted to avoid abnormal combustion. The design of the hydrogen injection system has been completed in a previous study [7]. There are two hydrogen injectors positioned at the cylinder's mid-stroke location, with a side angle and downward angle of both 10°CA, ensuring that the homogeneity of the hydrogen/air mixture can be guaranteed. The 3D geometric model of the LTMHE can be found in Figure 10(a).

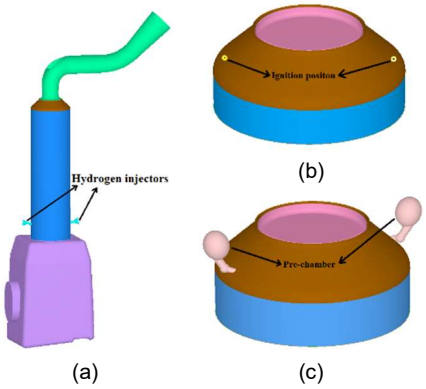

Figure 10.The 3D model of LTMHE.

The design of the LTMHE includes two parts: ignition position and ignition source. In terms of ignition position, in addition to the in-cylinder position where the nozzle of the prototype diesel injector is located (see Figure 10(b)), this study also discusses the position in the pre-chamber structure. Two pre-chambers were arranged on the cylinder head (see Figure 10(c)). On the other hand, two ignition methods were considered respectively: spark ignition and pilot diesel ignition. And the spark plug discharge time and injection timing of pilot diesel are both at 2°CA BTDC.

The flame propagation directions in the cylinder for the two ignition positions are similar. As shown in Figure 11, the high-temperature regions formed from ignition expand along the cylinder liner and towards the cylinder axis. The differences in combustion characteristics in different combustion systems are reflected in the flame propagation velocity. The ignition energy for pre-chamber ignition is determined by the jet flame generated in the pre-chamber. To obtain the optimal design of the combustion system for the LTMHE, the effects of different ignition energies on combustion characteristics for spark ignition and pilot diesel ignition are discussed separately in the cylinder and the pre-chamber.

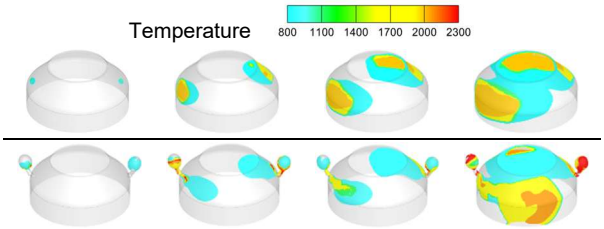

Figure 11. The ignition and combustion process without and with pre-chamber.

4.2 IGNITION IN CYLINDER

4.2.1 SPARK IGNITION IN CYLINDER

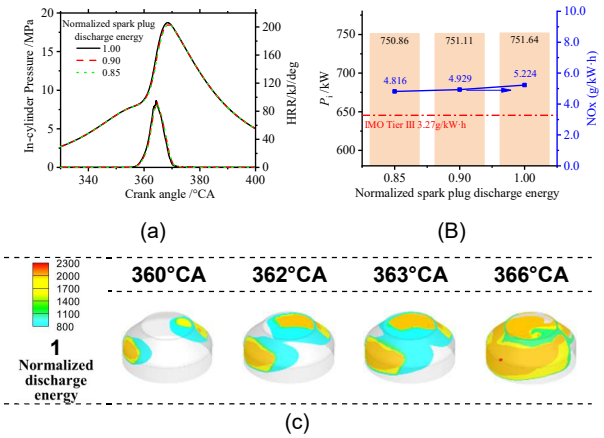

Figure 12. The comparison of combustion characteristics under different ignition energy for spark ignition in cylinder.

The variation in ignition energy of spark ignition in the cylinder has little impact on combustion characteristics. It can be seen in Figure 12(c) that the pressure curves and HRR curves almost coincide under different spark ignition energy. This indicates that the variation of spark plug ignition energy has negligible influence on the general IDTs. In all the operating conditions, the pre-mixture ignited by the spark plug burns rapidly resulting in high combustion temperatures and extensive high-temperature regions in the cylinder (see Figure 12(c)). As a result, the NOx emissions are significantly and exceed the IMO Tier III standard, as depicted in Figure 12(b). Furthermore, the maximum in-cylinder pressure surpasses 18.5 MPa, which poses a potential safety risk to the engine. To maintain consistency in the research, the ignition timing for the current spark ignition is set the same as the injection timing of pilot diesel

injection. However, unlike diesel pilot injection ignition, spark ignition does not involve physical processes like fuel spray breakup and evaporation, nor chemical IDTs. As a result, spark ignition initiates combustion of pre-mixture relatively earlier, leading to faster combustion and elevated combustion temperatures, which lead to higher NOx emissions. The ignition method using diesel pilot injection will be discussed in subsequent sections. Therefore, when spark ignition in the cylinder is adopted, the ignition timing should be carefully adjusted to avoid unqualified NOx emissions induced by combustion.

4.2.2 PILOT DIESEL IGNITION IN CYLINDER

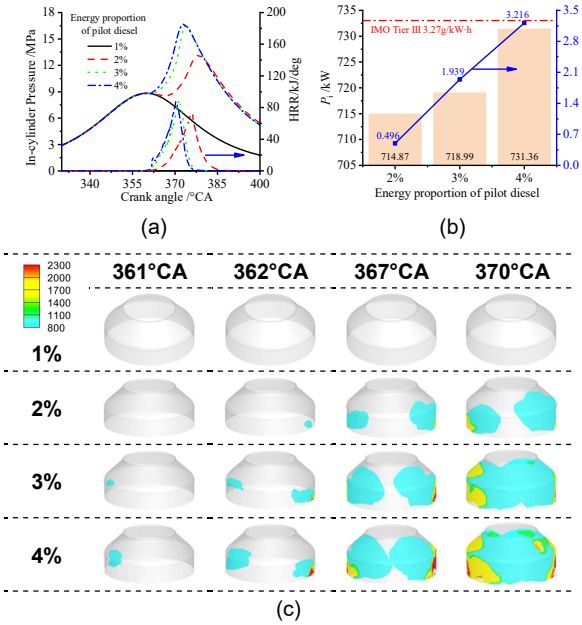

Figure 13. The comparison of combustion characteristics corresponding to different pilot diesel energy ratios without pre-chamber.

It can be seen from Figure 13 that the diesel energy proportion has a significant impact on combustion characteristics for pilot diesel ignition in the cylinder. When the energy proportion of pilot diesel is 1%, the ignition energy is not enough to ignite the lean pre-mixture. The flame propagation velocity increases as pilot diesel increases, which improves power performance, but deteriorates NOx emissions. When the energy proportion of pilot diesel is 2%, although the lean pre-mixture is ignited, the rate of pressure rise is relatively low, as seen in Figure 13(a). At this time, the maximum in-cylinder pressure is low (14.5 MPa) and the combustion duration is more than 25°CA. After increasing the energy proportion of pilot diesel to 3%, the flame velocity increases significantly and the combustion duration markedly reduces to 17°CA (see Figure 13(a) and (c)). Further increasing the energy proportion of pilot diesel causes little change in the pressure curve. The indicated power under the condition of 4% pilot diesel energy proportion is significantly larger compared to the other two schemes (see Figure 13(b)). However, the increase in combustion velocity also raises the combustion temperature, which results in more NOx emissions. The NOx emission of 4% pilot diesel energy proportion nearly reaches the limit of the IMO Tier III standard (see Figure 13(b)).

The reasonable pilot diesel energy proportion for in-cylinder ignition is 3%, with power performance approximately 90% of the prototype diesel engine and NOx emissions below the limit of IMO Tier III standard. It should be noted that the modification cost of this combustion system is relatively low among the schemes discussed, because the combustion chamber structure and diesel injectors of the prototype diesel engine can be used.

4.3 SPARK IGNITION IN PRE-CHAMBER

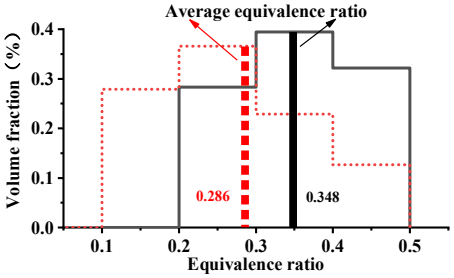

Figure 14. The comparison of the equivalence ratios in two pre-chambers before ignition.

The hydrogen injected into the cylinder during the gas exchange process continues to spread to the top of the cylinder with the swirl motion of fluid in the cylinder. The mass of hydrogen entering the two pre-chambers arranged in opposition is slightly different. As a result, the equivalence ratios in the two pre-chambers before ignition are different (0.286 and 0.348, see Figure 14). This difference might result in differences in the appearance time and combustion velocity of jet flames formed in the two pre-chambers.

4.3.1 SPARK IGNITION IN PRE-CHAMBER WITHOUT ENRICHED HYDROGEN INJECTION

Compared with spark ignition in the cylinder, for spark ignition in the pre-chamber, the variation of spark plug discharge energy has nearly no impact on either the pressure curve or the temperature distribution in the cylinder (see Figure 15(a) and (c)). Therefore, the indicated power and NOx emission are almost the same under four schemes. As shown in Figure 14, the equivalence ratio of pre-mixture in the pre-chamber is very low, so the energy of the jet flame formed in the pre-chamber

is low as well. Therefore, the appearance time of the jet flame in the main chamber is relatively later (about 2°CA ATDC). Furthermore, the flame propagation velocity is low because of the low energy of the jet flame, which leads to a slower in-cylinder pressure rise rate. Consequently, the maximum pressure of the four schemes is merely about 14 MPa, and the combustion duration is about 20°CA. On the other hand, thanks to the slow combustion, the high-temperature region is smaller, hence, the NOx emission is only about 20% of the IMO Tier III standard.

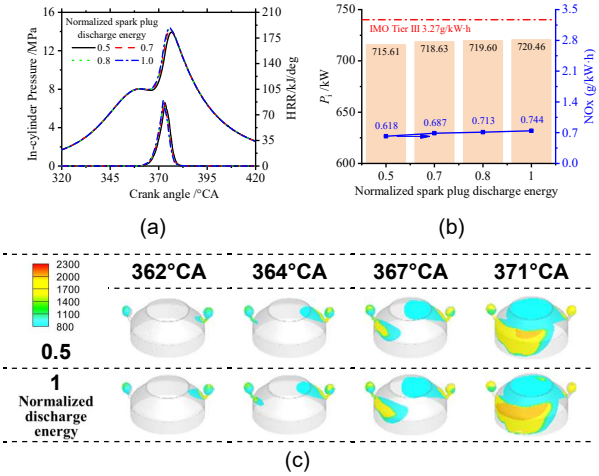

Figure 15. The comparison of combustion characteristics under different ignition energy for spark ignition in pre-chamber.

In summary, for spark ignition in the pre-chamber, due to the pre-mixture in the pre-chamber being too lean, the energy that the jet flame carries is relatively low. Considering its great potential in power performance and emission performance, measures are supposed to be taken to increase the jet flame energy.

4.3.2 SPARK IGNITION IN PRE-CHAMBER WITH ENRICHED HYDROGEN INJECTION

It can be seen from Figure 16(b) that the NOx emission for spark ignition in the pre-chamber is very low compared with the IMO Tier III limit. Therefore, there is great potential in improving the power performance. Furthermore, considering the equivalence ratio difference in the two pre-chambers, the enriched hydrogen injection in the pre-chamber before ignition was investigated. By adding two hydrogen high-pressure injectors in the two pre-chambers respectively and adjusting the injection mass individually, the equivalence ratios in the two pre-chambers are modified to be the same and increased simultaneously. The normalized discharge energy of the spark plug is set at 0.5. Before the enriched hydrogen injection, the equivalence ratios in the two pre-chambers are 0.286 and 0.348, respectively (see Figure 14).

Referring to the CVCC experiment in Section 3, increasing the concentration in the pre-chambers properly promotes combustion, resulting in higher jet flame intensity. The same conclusion can be drawn for pre-chamber spark ignition in LTMHE. Firstly, additional hydrogen is injected only into the pre-chamber with a leaner pre-mixture (the left one in Figure 16(c)), so that the equivalence ratios of the two pre-chambers are both 0.348. The jet flame from the left pre-chamber appears earlier than before, enhancing combustion in the main chamber. Further increasing the concentration in both pre-chambers not only leads to further promotion in power performance, but also increases NOx emissions. When the equivalence ratio reaches 0.5, NOx emissions exceed the IMO Tier III limit. Therefore, the equivalence ratio in the pre-chamber should not exceed 0.4 for spark ignition with enriched hydrogen injection in the pre-chamber.

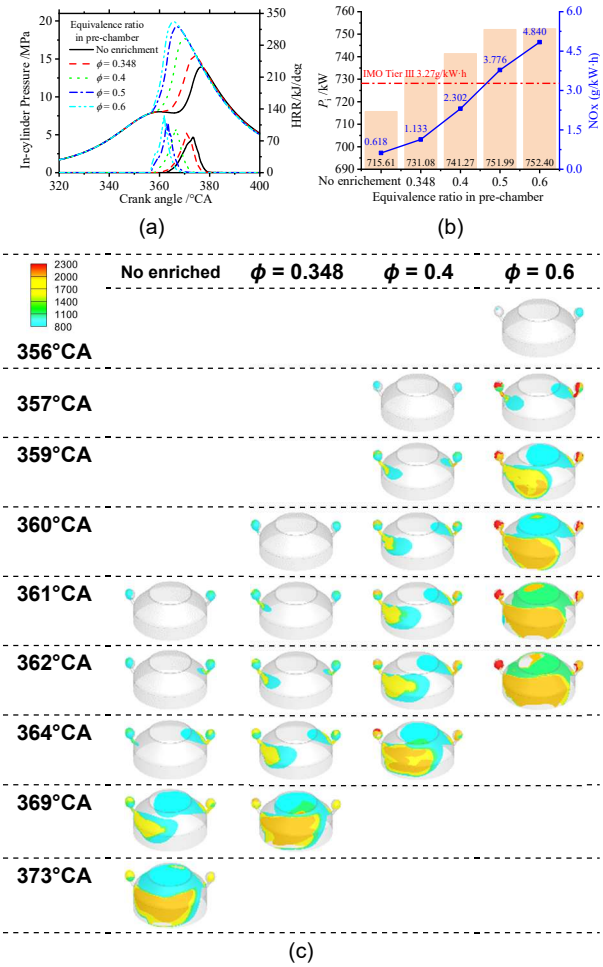

Figure 16. The influence of enrichment in pre-chamber on combustion characteristics under spark ignition in pre-chamber.

4.3.3 PILOT DIESEL IGNITION IN PRE-CHAMBER

Adopting pilot diesel ignition in the pre-chamber dramatically increases in-cylinder pressure. To ensure engine safety, the compression ratio is reduced to 12. Compared with pilot diesel ignition in the cylinder, a pilot diesel energy proportion of 1% for pre-chamber ignition successfully initiates combustion, which is one of the key advantages of the pre-chamber jet ignition system. At this point, the maximum in-cylinder pressure reaches 15.9 MPa. As seen in Figure 17(a), when the pilot diesel energy proportion increases to 2%, the maximum in-cylinder pressure rises by 3.4%. When the energy proportion reaches 3%, the maximum pressure increases to 16.8 MPa, and further increases in the pilot diesel proportion yield little change. Additionally, as the pilot diesel energy proportion increases, combustion duration shortens, and the peak heat release rate increases, while the ignition timing of the pre-mixture in the cylinder remains relatively unchanged. The higher combustion velocity enlarges the high-temperature regions, as shown in Figure 17(c). Consequently, NOx emissions increase as the pilot diesel energy proportion rises. However, Figure 17(c) shows that reducing the pilot diesel proportion not only enhances power performance but also increase NOx emissions. The diesel energy proportion of 1% is the optimal choice for pilot diesel ignition in the pre-chamber, achieving nearly 90% of the prototype diesel engine's power output, with NOx emissions at just 27% of the IMO Tier III limit.

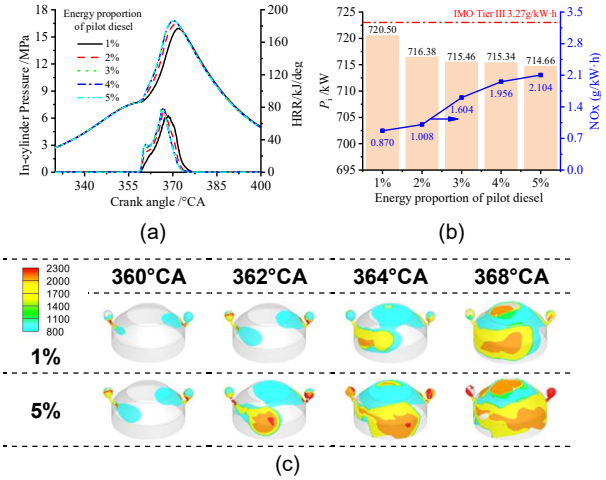

Figure 17. The comparison of combustion characteristics corresponding to different pilot diesel energy ratios with pre-chamber.

5 CONCLUSIONS

This study investigates the ignition delay times (IDTs) of hydrogen-heptane, hydrogen/iso-octane, and hydrogen/PRF mixtures under varying temperatures (600 K – 1000 K) and pressures (8 bar, 16 bar, and 24 bar) using a rapid compression machine (RCM). A multi-objective genetic algorithm was employed to develop a skeletal hydrogen/PRF mechanism, which accurately predicts the experimental IDT values. Additionally, the hydrogen jet flame characteristics were studied in an optical constant volume combustion chamber (CVCC). The impact of the equivalence ratio in the pre-chamber on the hydrogen jet flame behavior was analyzed, and the CFD simulation models were validated through experimental images and pressure curves.

The combustion system of the LTMHE was designed and optimized through numerical simulations, utilizing the developed skeletal hydrogen/PRF mechanism and insights from the CVCC experiments. The results indicate that though ignition in the cylinder leads to efficient and stable combustion, it also causes rapid combustion, which tends to result in relatively high NOx emissions. By utilizing a pre-chamber, the flammable limit of the lean pre-mixture can be widened, the flame propagation speed can be increased, and combustion variability can be improved. Additionally, the risk of excessively high combustion temperatures can be mitigated, offering significant potential for enhancing power performance while controlling NOx emissions.

Increasing the combustion intensity in the pre-chamber—via methods such as enhancing spark plug ignition energy, increasing pilot diesel energy proportion, and enriching hydrogen injection—can improve jet flame combustion. In LTMHEs, the pre-mixture in the pre-chamber is extremely lean due to the low rotational speed and large cylinder space. Therefore, enhancing the ignition energy in the pre-chamber, such as through enriched injection or pilot diesel ignition, is necessary for effective ignition.

Looking ahead, in light of increasingly stringent emission regulations, pilot diesel ignition in the pre-chamber holds great promise due to its potential to significantly reduce NOx emissions.

6 ACKNOWLEDGMENTS

This work was supported by the Natural Science Foundations of China [grant number 52471315], [grant number 52071061]; and the Research on combustion key technology of Otto-cycle ammonia engine combustion.

7 REFERENCES AND BIBLIOGRAPHY

[1] H. Li and G. A. Karim, Knock in spark ignition hydrogen engines, *International Journal of Hydrogen Energy,* vol. 29, no. 8, pp. 859-865, 2004.

[2] M. A. R. S. Al-Baghdadi, Effect of compression ratio, equivalence ratio and engine speed on the performance and emission characteristics of a spark ignition engine using hydrogen as a fuel, *Renewable Energy,* vol. 29, no. 15, pp. 2245-2260, 2004.

[3] A. Menaa, M. S. Lounici, F. Amrouche, K. Loubar, and M. Kessal, CFD analysis of hydrogen injection pressure and valve profile law effects on backfire and pre-ignition phenomena in hydrogen-diesel dual fuel engine, *International Journal of Hydrogen Energy,* vol. 44, no. 18, pp. 9408-9422, 2019.

[4] L. Rouleau, F. Duffour, B. Walter, R. Kumar, and L. Nowak, Experimental and numerical investigation on hydrogen internal combustion engine, SAE Technical Paper0148-7191, 2021.

[5] Y. Lu, J. Que, M. Liu, H. Zhao, and L. Feng, Study on backfire characteristics of port fuel injection single-cylinder hydrogen internal combustion engine, *Applied Energy,* vol. 364, p. 123110, 2024.

[6] Z. Wang, M. Song, H. Zhao, Y. Lu, Z. Gong, and L. Feng, Investigation of the hydrogen pre-ignition induced by the auto-ignition of lubricating oil droplets, *Applied Thermal Engineering,* vol. 259, p. 124927, 2025.

[7] W. Qu *et al.*, Hydrogen injection optimization of a low-speed two-stroke marine hydrogen/diesel engine, *Fuel,* vol. 366, p. 131352, 2024.

[8] E. Toulson, H. C. Watson, and W. P. Attard, Gas assisted jet ignition of ultra-lean LPG in a spark ignition engine, SAE Technical Paper0148-7191, 2009.

[9] W. P. Attard and P. Parsons, Flame kernel development for a spark initiated pre-chamber combustion system capable of high load, high efficiency and near zero NOx emissions, *SAE International Journal of Engines,* vol. 3, no. 2, pp. 408-427, 2010.

[10] K. Yamanaka, Y. Shiraga, and S. Nakai, Development of pre-chamber sparkplug for gas engine, SAE Technical Paper0148-7191, 2011.

[11] Y.-D. Liu, M. Jia, M.-Z. Xie, and B. Pang, Enhancement on a Skeletal Kinetic Model for Primary Reference Fuel Oxidation by Using a Semidecoupling Methodology, *Energy & Fuels,* vol. 26, no. 12, pp. 7069-7083, 2012.

[12] Z. Wang, D. Zhang, Y. Fang, M. Song, Z. Gong, and L. Feng, Experimental and numerical investigation of the auto-ignition characteristics of cylinder oil droplets under low-speed two-stroke natural gas engines in-cylinder conditions, *Fuel,* vol. 329, p. 125498, 2022.

[13] Z. Gong, M. Hu, Y. Fang, D. Zhang, and L. Feng, Mechanism study of natural gas pre-ignition induced by the auto-ignition of lubricating oil, *Fuel,* vol. 315, p. 123286, 2022.

[14] M. Song *et al.*, Auto-ignition characteristics and chemical reaction mechanism of ammonia/n-heptane mixtures with low n-heptane content, *Fuel,* vol. 364, p. 131011, 2024.

[15] D. G. Goodwin, H. K. Moffat, and R. L. Speth, Cantera: An object-oriented software toolkit for chemical kinetics, thermodynamics, and transport processes, ed: version, 2018.

[16] L. Elliott, D. B. Ingham, A. G. Kyne, N. S. Mera, M. Pourkashanian, and C. W. Wilson, Genetic algorithms for optimisation of chemical kinetics reaction mechanisms, *Progress in Energy and Combustion Science,* vol. 30, no. 3, pp. 297-328, 2004/01/01/ 2004.

[17] J. Tian, Z. Cui, Z. Ren, H. Tian, and W. Long, Experimental study on jet ignition and combustion processes of natural gas, *Fuel,* vol. 262, p. 116467, 2020.

[18] D. Dong *et al.*, Optical investigation of ammonia rich combustion based on methanol jet ignition by means of an ignition chamber, *Fuel,* vol. 345, p. 128202, 2023.

[19] X. Meng *et al.*, Understanding of combustion characteristics and NO generation process with pure ammonia in the pre-chamber jet-induced ignition system, *Fuel,* vol. 331, p. 125743, 2023.

[20] F. Wei, Y. Wang, H. Tian, J. Tian, W. Long, and D. Dong, Visualization study on lean combustion characteristics of the premixed methanol by the jet ignition of an ignition chamber, *Fuel,* vol. 308, p. 122001, 2022.

[21] C. R. Nave, Hydrogen spectrum, *HyperPhysics. Georgia State University,* 2006.

[22] Q. Zhang, Y. Qi, R. Zhang, X. Chao, B. Yang, and Z. Wang, Chemiluminescence spectra investigation of ammonia flame over a wide-range equivalence ratios in a rapid compression machine, *Fuel,* vol. 382, p. 133604, 2025.

[23] F. Wei *et al.*, Optical experiment study on Ammonia/Methanol mixture combustion performance induced by methanol jet ignition in a

constant volume combustion bomb, *Fuel,* vol. 352, p. 129090, 2023.

[24] H. Yu, J. Chen, S. Duan, P. Sun, W. Wang, and H. Tian, Effect of natural gas injection timing on performance and emission characteristics of marine low speed two-stroke natural gas/diesel dual-fuel engine at high load conditions, *Fuel,* vol. 314, p. 123127, 2022.

[25] H. Yu, W. Wang, D. Sheng, H. Li, and S. Duan, Performance of combustion process on marine low speed two-stroke dual fuel engine at different fuel conditions: Full diesel/diesel ignited natural gas, *Fuel,* vol. 310, p. 122370, 2022.

[26] W. Jin, H. Gan, Y. Cong, and G. Li, Performance optimization and knock investigation of marine two-stroke pre-mixed dual-fuel engine based on RSM and MOPSO, *Journal of Marine Science and Engineering,* vol. 10, no. 10, p. 1409, 2022.

[27] L. Zhu *et al.*, Effects of fuel reforming on large-bore low-speed two-stroke dual fuel marine engine combined with EGR and injection strategy, *International Journal of Hydrogen Energy,* vol. 45, no. 53, pp. 29505-29517, 2020.

[28] L. Liu, Y. Wu, Q. Xiong, and T. Liu, Analysis on flow motion and combustion process in pre-chamber and main chamber for low-speed two-stroke dual-fuel engine, SAE Technical Paper0148-7191, 2019.